

FABRICATION OF ELECTROCHEMICAL ELECTRODES BASED ON PLATINUM AND ZnO NANOFIBERS FOR BIOSENSING APPLICATIONS

DANG THI THANH LE^{a,†}, NGUYEN VAN HOANG^a, NGUYEN VAN HIEU^a,
VU QUANG KHUE^b, TRAN QUANG HUY^c, AND MATTEO TONEZZER^d

^a*International Training Institute for Materials Science (ITIMS), Hanoi University of Science and Technology (HUST), No.1, Dai Co Viet Str., Hanoi, Vietnam*

^b*Advanced Institute for Science and Technology (AIST), Hanoi University of Science and Technology (HUST), No.1, Dai Co Viet Str., Hanoi, Vietnam*

^c*National Institute of Hygiene and Epidemiology (NIHE), 1- Yersin Street, Hanoi, Vietnam*

^d*IMEM-CNR, sede di Trento - FBK, Via alla Cascata 56/C, Povo - Trento, Italy*

[†]*E-mail: thanhle@itims.edu.vn*

Received 09 July 2016

Accepted for publication 31 August 2017

Published 19 September 2017

Abstract. *Platinum (Pt) electrodes were designed in imitation of screen-printed electrodes, and prepared by microelectronic techniques. These electrodes were then modified with zinc oxide (ZnO) nanofibers for biosensing applications. ZnO nanofibers with average length $\sim 20\text{-}30\ \mu\text{m}$ and diameter $\sim 150\ \text{nm}$ in hexagonal crystalline structure are prepared using electrospinning method. Their surface characteristics were analyzed by field emission scanning electron microscopy, energy-dispersive X-ray spectroscopy, and X-ray diffraction. Electrochemical properties of modified Pt electrodes were investigated in comparison with commercial carbon screen-printed electrodes. The results showed that the cyclic voltammogram of modified Pt electrodes was stable, but has much lower resistance compared to that of carbon screen-printed electrodes.*

Keywords: biosensing, nanofibers, electrochemical Pt electrodes, ZnO.

Classification numbers: 87.85.fk, 82.45.Fk, 82.45.Tv, 87.15.Tt.

I. INTRODUCTION

The development of electrochemical sensors has attracted a great deal of interest due to their high sensitivity and selectivity, and they are being increasingly used in many fields, such as

analytical chemistry, industrial process monitoring and control, clinical diagnostics, environmental monitoring and security, and food safety [1].

Metal oxide semiconductors have been attracting much attention in point-of-care diagnostics because of their wide range of conductivity, high biological activity, and enhanced sensitivity. The bioconjugation of protein molecules with a metal oxide surface has been recently developed for point-of-care (POC) diagnostics devices [2]. Among them, zinc oxide (ZnO) is very attractive due to its chemical and thermal stability, its good biocompatibility, higher diffusion coefficient and electron mobility [3–7]. ZnO is a well-known n-type, direct wide-band-gap II–VI semiconductor with a band gap of 3.37 eV, high electron mobility ($210 \text{ cm}^2 \cdot \text{V}^{-1} \cdot \text{s}^{-1}$) and a large excitonic binding energy of 60 meV at room temperature [8]. High isoelectric point (IEP=9.5) of zinc oxide nanomaterials enables them to easily be bound electrostatically with the low isoelectric point protein molecules (IEP \sim 1 – 5) [9]. ZnO has a wide range of applications in optoelectronics, sensors, transducers, energy conversion and medical sciences. The anisotropic structure of ZnO is known to exhibit higher electron mobility and diffusion coefficient compared to other metal oxides like titanium oxide [10]. Thus, there has been a rapid growth in the literature concerning the application of ZnO for the detection of various biomolecules such as glucose, DNA, antibodies and bacteria with improved stability and selectivity [11]. One-dimensional (1D) ZnO-NFs, which boost surface-to-volume ratio and have a high electron mobility, provide a direct and stable pathway for rapid electron transport. This results in higher sensitivity of the biodevices and makes them a very promising material for immobilization of biomolecules without electron mediator for use in electrochemical immunosensor [12, 13].

Among the various synthesizing processes of 1D nanostructures, electrospinning is a simple, robust, low cost and versatile method of producing nanofibers in a large scale [14]. The porous structure of the nanomaterials could provide a large surface area for more protein binding per planar area unit, and for higher protein entrapment, resulting in higher sensitivity.

Screen-printed electrodes are frequently used in analytical applications because of their unique properties such as small size, low detection limit, fast response time, high reproducibility, etc. [15]. To our surprise we find there are very few literature reports concerning the fabrication of platinum screen printed electrodes; consequently in this paper we use platinum pseudo-screen-printed electrodes [15–18]. Platinum is an electrode which has been successfully utilized for the offering of faster electrode kinetics over that of the traditional, more sluggish carbon based electrodes. Drawbacks to the use of a traditional platinum electrode evidently centre on the expense and uneconomical nature of such materials.

In this work, we demonstrate nanofibers-modified Pt/SiO₂/Si substrate which could be used as point-of-care diagnostic platform for immunosensing applications. A simple, low cost, electrospinning method was used to synthesize zinc oxide nanofibers. The synthesized nanofibers matrix was electrophoretically deposited onto Pt/SiO₂/Si substrate. The comparison on electrochemical properties between carbon screen-printed electrodes (SPEs) and platinum electrodes was discussed.

II. EXPERIMENTAL

Material preparation

The ZnO nanofibers were synthesized by electrospinning followed by calcination. Zinc (II) acetate $\text{Zn}(\text{CH}_3\text{COO})_2 \cdot 2\text{H}_2\text{O}$ and polyvinyl alcohol (PVA, molecular weight = 130'000) were purchased from Aldrich and used as received without any further purification. All the chemicals are analytical grade.

In a typical experiment, firstly a 2 g PVA was dissolved in 18 mL of deionized water at 70°C by stirring for 6 h, then 1 g of zinc acetate ($\text{Zn}(\text{CH}_3\text{COO})_2 \cdot 2\text{H}_2\text{O}$) was added to the above solution. This mixture was continuously stirred for 6 h at 70°C leading to the formation of a transparent zinc hydroxide/PVA sol. The as-prepared sol was transferred to a 10 mL syringe with a hypodermic needle (diameter 27G) and inserted in a controlled electrospinning setup (Electrospunra, Singapore). The obtained optimal conditions for electrospun nanofibers were flow rate of 0.2 mL/h and applied electric field of 18 kV/cm. The fiber mat was harvested and annealed at 500°C for 1 h to yield ZnO nanofibers. The heating and cooling ramps during sintering process were kept at 100°C/1 hour.

Sensor fabrication

The electrochemical 3-legs electrodes were designed for biosensing applications based on commercial screen-printed carbon electrodes. 20 nm Cr and 150 nm Pt were deposited on a 4 inch silicon wafer covered with 300 nm of SiO_2 using a sputtering system. To fabricate the electrodes with 136 mm² areas, Pt and Cr were patterned via photolithography and lifting-off. One 4 inch silicon wafer was diced to fabricate 41 rectangular devices with dimensions of 8×17 mm. The image of Pt and commercial electrodes was shown in Fig. 1.

ZnO nanofibers (NFs) synthesized on Pt/ SiO_2 substrate are used as the working electrode. The electrochemical sensors were fabricated with the electrospun nanofibers.

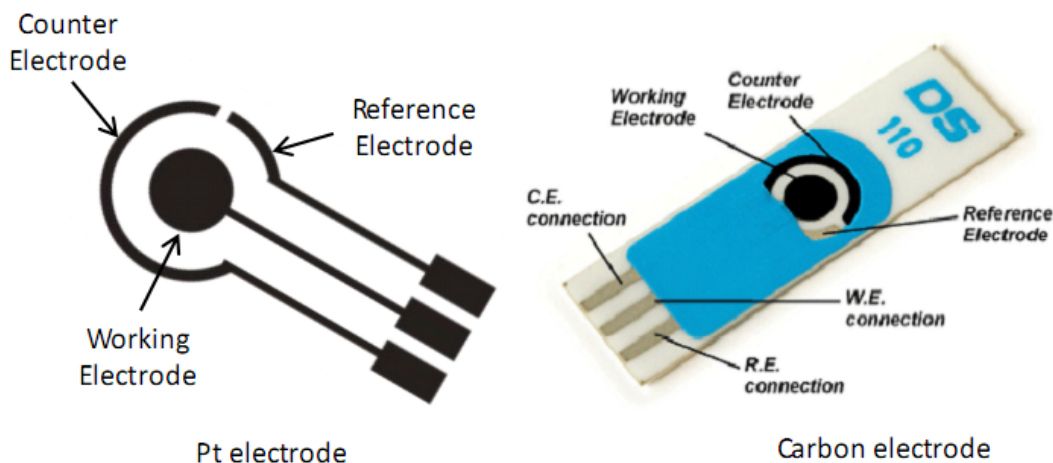


Fig. 1. Pt and commercial carbon electrodes.

Experimental characterizations of the electrode

Structure, morphology and composition of the as-synthesized ZnO nanofibers were characterized by X-ray diffraction (XRD, D8 Advance, Bruker), energy dispersion spectroscopy (EDS) and field emission scanning electron microscopy (FESEM, S-4800, Hitachi). Cyclic voltammetry (CV) and electrochemical impedance spectroscopy (EIS) measurements were carried out on an instrument PalmSens 3 consisting of a microprocessor and a low noise and low-current potentiostat/galvanostat in PBS solution (50 mM, pH 7.4, 0.9% NaCl) containing 5 mM $[\text{Fe}(\text{CN})_6]^{3-/4-}$.

The CV measurements were performed scanning from -0.9 to +0.9 V at a scan rate of 100 mV/s to evaluate the modification of Pt electrode with ZnO NFs. For the comparison study, bare (unmodified) Pt electrodes were also used. The EIS spectra were recorded at an equilibrium potential without external biasing in the frequency range of $0.001 \div 5 \times 10^4$ Hz in an open-circuit potential value of +0.0 V with a 10 mV amplitude.

III. RESULTS AND DISCUSSION

Comparison of electrochemical properties between SPEs and Pt electrodes

Compared to cyclic voltammogram of commercial carbon screen-printed electrodes (SPEs), cyclic voltammograms of platinum electrodes are almost similar with low resistance as shown in Fig. 2. Figure 2 shows the cyclic voltammograms of oxidation/reduction of 5 mM $[\text{Fe}(\text{CN})_6]^{3-/4-}$ redox probe using a scan rate of 100 mV/s for bare Pt-electrodes (back line) and bare SPEs (red line). As we can see, they have the congruent shape but lower resistance of platinum electrodes.

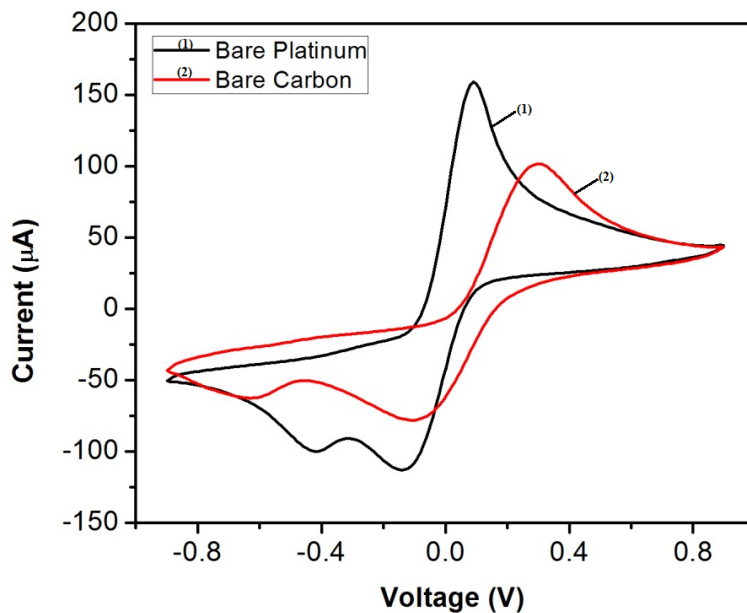


Fig. 2. Cyclic voltammograms of SPEs (1) and platinum electrodes (2).

In parallel, compared to impedance spectrum of commercial carbon screen-printed electrodes (SPEs), impedance spectra of platinum electrodes are almost similar with low resistance as shown in Fig. 3. The impedance spectrum of SPEs has much bigger semicircle diameter, further confirming the much lower resistance of platinum electrodes.

The as-prepared platinum electrodes were used to deposit ZnO NFs for the investigation of electrochemical properties.

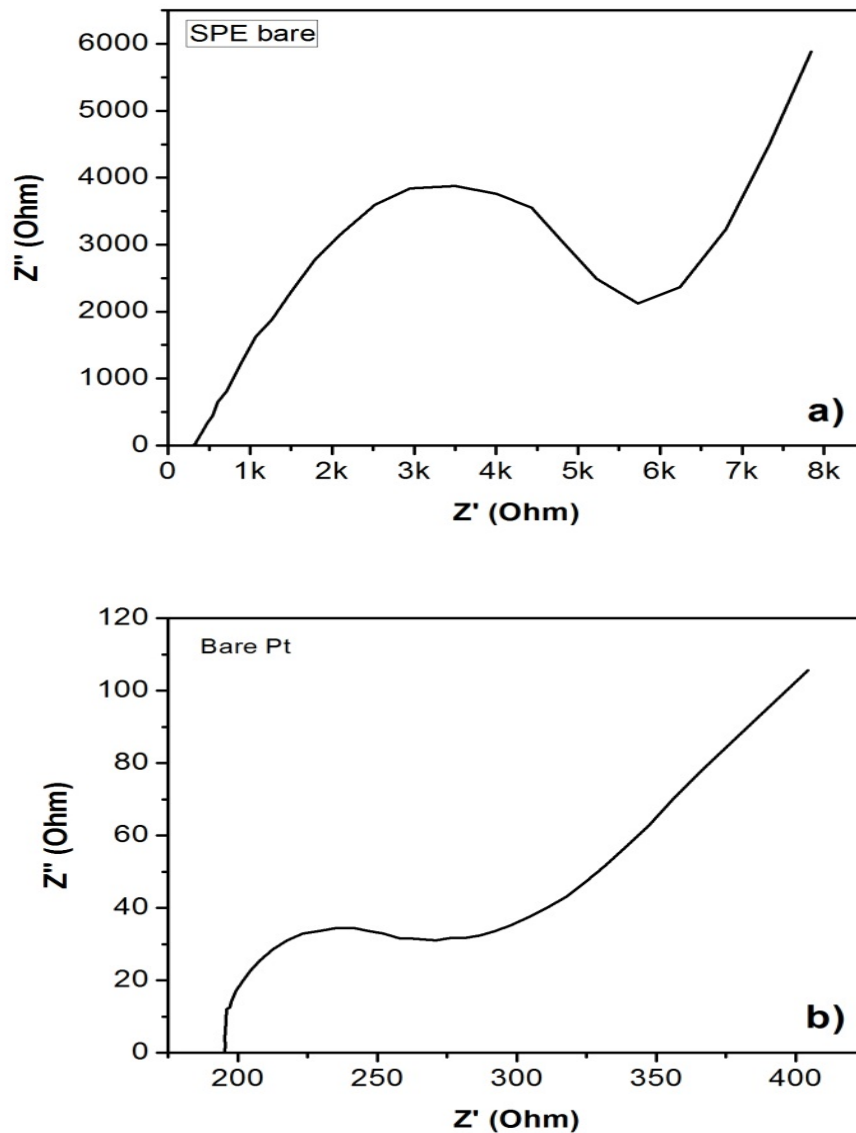


Fig. 3. Nyquist plots of SPE (a) and platinum electrodes (b).

Material characterization

After calcination, the as-spun fibers exhibited an average diameter of ~ 150 nm and were distributed randomly but uniformly over the silicon substrate as shown in Fig. 4. The diameter and morphology of the fibers could be controlled either by decreasing the applied voltage, process temperature or by increasing the molecular weight of the precursors.

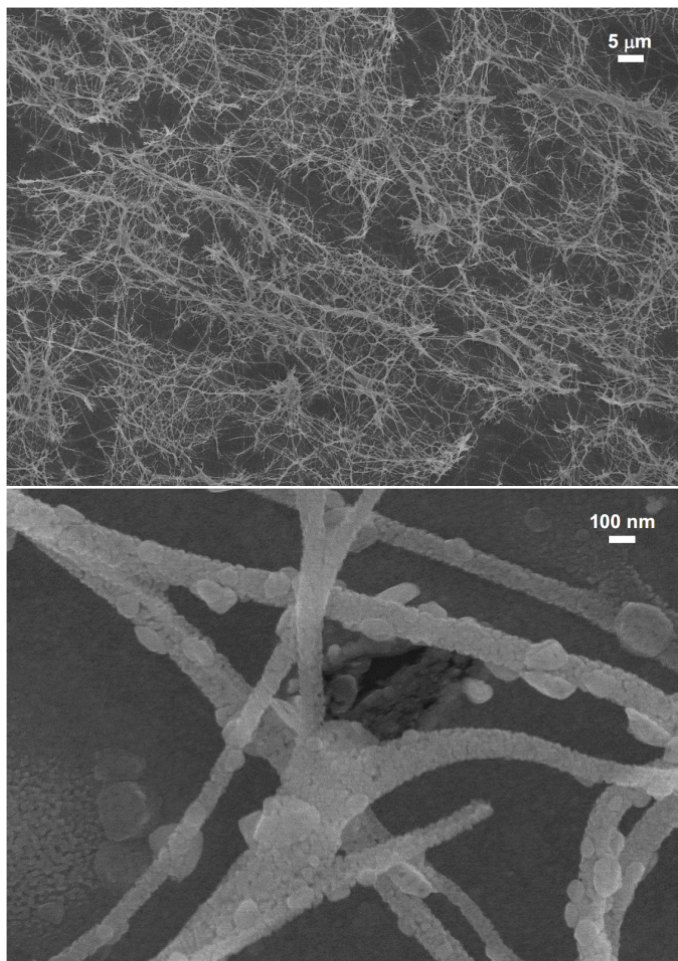


Fig. 4. FE-SEM images of ZnO nanofibers prepared by electrospinning at different magnifications.

In order to investigate the composition of the electrospun nanofibers, energy dispersion spectroscopy was used, and a typical spectrum is shown in Fig. 5. It is evident that the nanofibers are composed of zinc oxide, containing Zn and O. The peaks of Si and Pt indicated that the EDS analysis was done on electrode covered by ZnO NFs. All of the investigated nanofibers show a stoichiometry poor in oxygen, as expected by ZnO nanosized grains in which the surface greatly affects the overall composition.

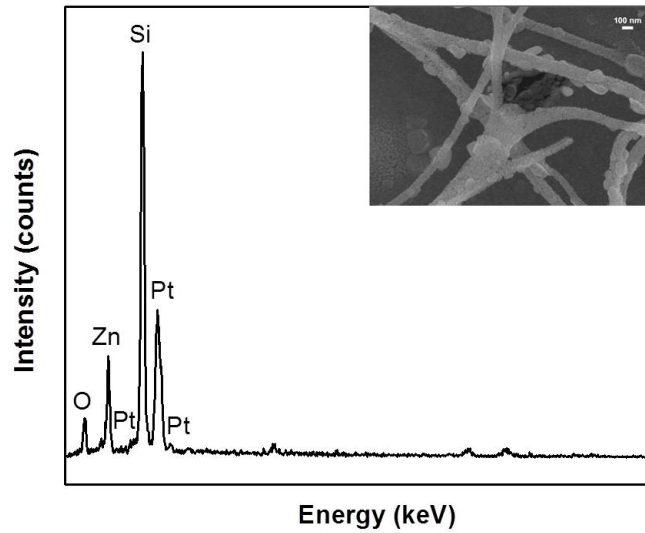


Fig. 5. EDS spectrum of ZnO nanofibers prepared by electrospinning.

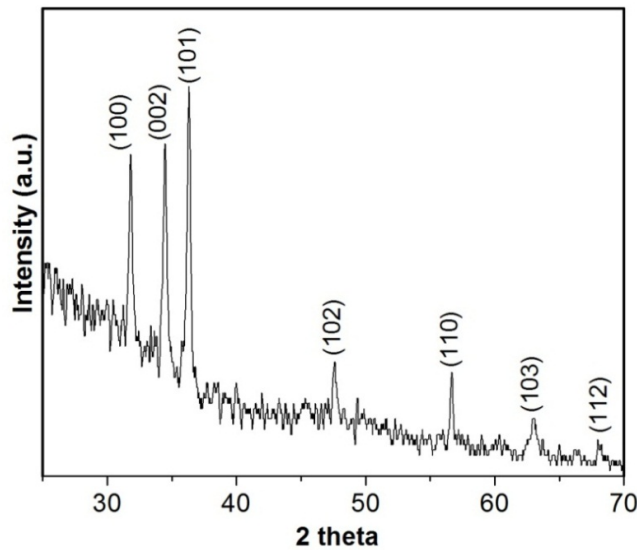


Fig. 6. XRD analysis of the ZnO nanofibers.

The structure of the deposited material was then investigated by x-ray diffraction, and a typical spectrum is illustrated in Fig. 6. The common peaks at 31.86° , 34.49° , 36.34° , 47.63° , 56.65° , 62.96° and 68.04° correspond to ZnO wurtzite structure crystal planes (100), (002), (101),

(102), (110), (103), and (112), in agreement with JCPDS card no. 36-1451 (lattice parameters: a , $b = 3.249 \text{ \AA}$ and $c = 5.206 \text{ \AA}$) [8, 19]. No peak from impurities has been found.

Electrochemical properties

The electron transfer behavior, before and after surface modification of the Platinum electrodes with ZnO NFs, was investigated by cyclic voltammetry. Figure 7 shows the cyclic voltammograms of oxidation/reduction of 5 mM $[\text{Fe}(\text{CN})_6]^{3-/4-}$ redox probe using a scan rate of 100 mV/s for bare Pt-electrode (Fig. 7a) and Pt/ZnO NFs (Fig. 7b). As can be seen, the bare Pt-electrode exhibited a well defined Faradaic current response for $[\text{Fe}(\text{CN})_6]^{3-/4-}$, indicating the diffusion-controlled electron transfer at the bare Pt-electrode surface. As the electrode covered by ZnO NFs, the magnitude of the electrochemical current response is decreased owing to the semiconducting nature of ZnO NFs matrix on Pt-electrode.

Electrochemical impedance spectroscopy (EIS) recently has attracted much interest because it has some important advantages over number of electrochemical methods such as amperometry and potentiometry. With EIS, developed sensing platforms are (i) label-free with detection based on direct specific binding events, (ii) less destructive to the activities of biomolecule due to the small voltage excitation used during detection, (iii) simple operating and very sensitive, with comparable detection limits to optical-based sensors [20]. In impedimetric sensors, detection is based on the principle that any substance attached on the electrode will change the measured impedance. Therefore, any change in the impedance spectra can be related to the change of interface properties.

In the present work, Nyquist plots were used to investigate the change in electron transfer resistance at the interface between the sensor and the redox probe solution after depositing ZnO nanofibers.

In general, the complex impedance is displayed in two parts including a semicircle (at high frequencies, corresponding to the electron transfer limited process) and a linear part (at lower frequencies resulting from the diffusion limiting step of the electrochemical process). The change in the semicircle diameter is a result of the change in the interfacial electron transfer resistance (R_{CT}); that is, the resistance corresponding to the carrier transfer from the modified electrode to the ferricyanide in the solution. Thus, the observed diameter increase is explained as the semiconducting property of ZnO material.

The electrochemical characterization of bare Pt electrode and ZnO NFs/Pt was then performed using EIS technique. The corresponding Nyquist plots are shown in Fig. 8. This figure represents the Nyquist diagram of the electrodes prepared at two stages of surface modifications. As can be seen, the bare Pt-electrode (red line) showed a lower semicircle domain indicating a very low resistance to the $[\text{Fe}(\text{CN})_6]^{3-/4-}$ redox probe. When the bare Pt-electrode was modified with ZnO NFs matrix, the diameter of the semicircle portion increased remarkably (black line), indicating the semiconducting nature of ZnO matrix at the electrode interface. The result is complementary to cyclic voltammetry measurements, further confirming the successful fabrication step of the electrochemical sensors for detection of biomolecules.

The platform developed in our work provided some important advantages, such as practical fabrication, simplicity in use by requiring less consumables/chemicals. Excluding the fabrication process of ZnO NFs/Pt, each CV and EIS measurement was completed only in 4 and 20 min, respectively.

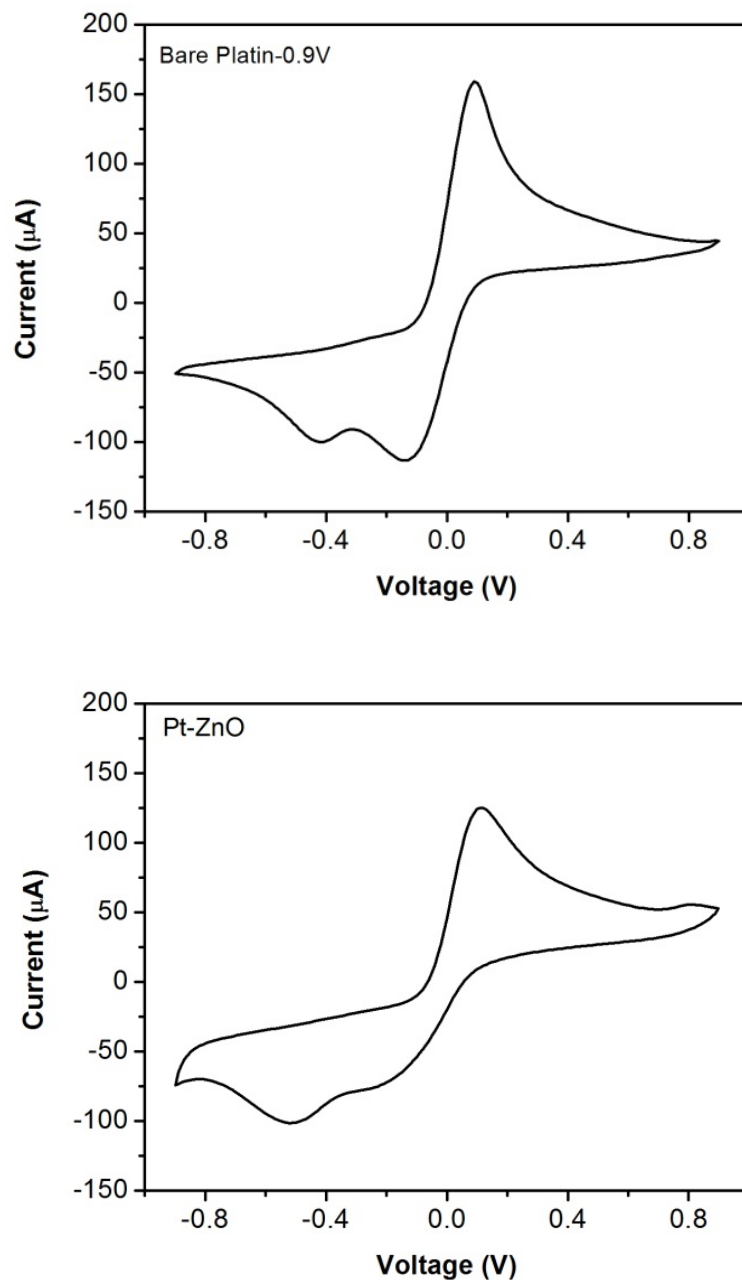


Fig. 7. Cyclic voltammograms of a) bare platinum electrode and b) after growth of ZnO NFs.

As we know, the R_{CT} value of Pt electrodes is very small. When Pt WE was modified with ZnO NFs, R_{CT} value will be increased because of semiconducting nature of ZnO. In addition,

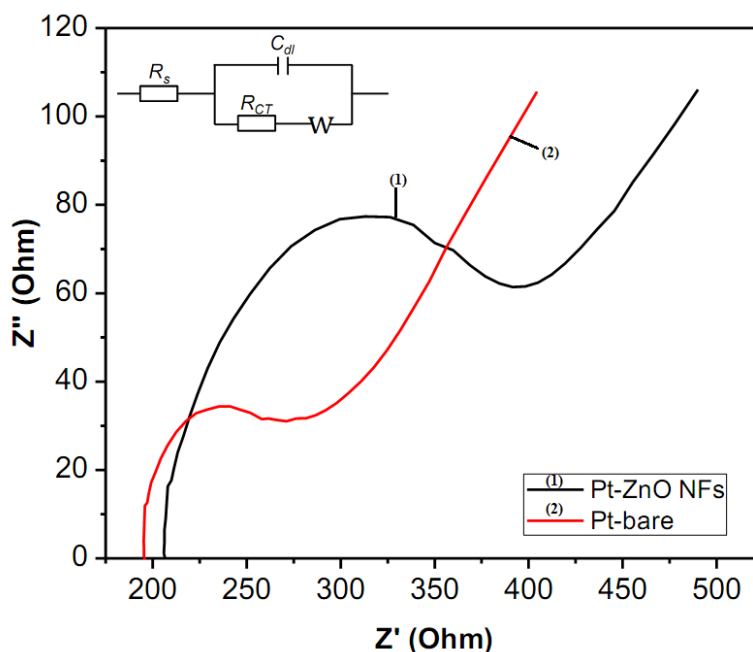


Fig. 8. Nyquist plots obtained of bare platinum electrode (red line) and after deposition of ZnO NFs (black line). Inset: The Randles equivalent circuit model.

when being modified with ZnO nanostructures (NFs), the surface area of WE will be significantly increased leading to the large number of bio-recognition probes immobilized on the WE, it also means that the modified Pt electrodes will be more sensitive.

IV. CONCLUSION

Electrochemical Pt electrodes based on ZnO nanofibers matrix have been successfully prepared through the electrospinning method for the aim of detecting biomolecules. The matrix was consisting of ZnO nanofiber of average length $\sim 20\text{-}30\ \mu\text{m}$ and diameter $\sim 150\ \text{nm}$ with hexagonal crystalline structure. The modified platinum electrodes showed much lower resistance compared to SPEs. We believe that the electrochemical Pt electrodes and ZnO NFs/Pt hold great potential for biosensing applications. In addition, due to the stability of their electrochemical properties, ZnO NFs-modified Pt electrodes also reveal their potential to be utilized in lab-on-a-chip technologies.

ACKNOWLEDGEMENTS

This research is funded by Vietnam National Foundation for Science and Technology Development (NAFOSTED) under grant number 103.02-2015.43. It is also supported by the research project between Vietnam and Italy, coded NDT.05.ITA/15.

REFERENCES

- [1] Z. H. Yang, Y. Zhuo, R. Yuan, Y. Q. Chai, *Biosensors and Bioelectronics* **78** (2016) 321.
- [2] P. Si, S. Ding, J. Yuan, X. W. D. Lou and D. -H. Kim, *ACS Nano* **5** (2011) 7617.

- [3] K. Mondal, M. A. Ali, V. V. Agrawal, B. D. Malhotra and A. Sharma, *ACS Applied Materials & Interfaces* **6** (2014) 2516.
- [4] M. Ahmad, C. Pan, Z. Luo and J. Zhu, *Journal of Physical Chemistry C* **114** (2010) 9308.
- [5] Y. Fang, Q. Pang, X. Wen, J. Wang and S. Yang, *Small* **2** (2006) 612.
- [6] H. Hong, J. Shi, Y. Yang, Y. Zhang, J. W. Engle, R. J. Nickles, X. Wang and W. Cai, *NanoLetters* **11** (2011) 3744.
- [7] P. K. Vabbina, A. Kaushik, N. Pokhrel, S. Bhansali and N. Pala, *Biosensors and Bioelectronics* **63** (2015) 124.
- [8] M. Tonezzer, D. T. T. Le, N. Bazzanella, N. V. Hieu, S. Iannotta, *Sensors and Actuators B* **220** (2015) 1152.
- [9] P. R. Solanki, A. Kaushik, V. V. Agrawal and B. D. Malhotra, *NPG AsiaMaterials* **3** (2011) 17.
- [10] S. S. Mali, H. Kim, W. Y. Jang, H. S. Park and P. S. Patil, *ACS Sustainable Chemistry & Engineering* **1** (2013) 1207.
- [11] J. Liu, P. Pham, V. Haguët, F. Sauter-Starace, L. Leroy, A. Roget, E. Descamps, A. Bouchet, A. Buhot, P. Mailley and T. Livache, *Analytical Chemistry* **84** (2012) 3254.
- [12] K. Brinze Paul, S. Kumar, S. Tripathy, S. R. Vanjari, V. Singh, S. G. Singh, *Biosensors and Bioelectronics* **80** (2016) 39.
- [13] J. Wua, F. Yin, *Sensors and Actuators B* **185** (2013) 651.
- [14] N. V. Dung, D. T. T. Le, N. D. Trung, H. N. Dung, N. M. Hung, N. V. Duy, N. D. Hoa, N. V. Hieu, *Journal of Nanoscience and Nanotechnology* **16** (2016) 7910.
- [15] Ivanildo Luiz de Mattos, Lo Gorton, Tautgirdas Ruzgas, *Biosensors and Bioelectronics* **18** (2003) 193-200.
- [16] J. P. Metters, F. Tan, R. O. Kadara and C. E. Banks, *Analytical Methods* **4** (2012) 1272.
- [17] L. del Torno-de Román,; M. A. Alonso-Lomillo, O. Domínguez-Renedo, C. Merino-Sánchez, M. P. Merino-Amayuelas, M. J. Arcos-Martínez, *Talanta* **86** (2011) 324.
- [18] P. Dutronc, B. Carbonne, F. Menil and C. Lucat, *Sensors and Actuators B* **6** (1992) 279.
- [19] V. Perumal, U. Hashim, Subash C. B. Gopinath, R. Haarindradas, K. L. Foo, S. R. Balakrishnan & P. Poopalan, *Scientific Reports* **5** (2015) 12231.
- [20] T. T. N. Lien, Y. Takamura, E. Tamiya and M. C. Vestergaard, *Analytica Chimica Acta* **892** (2015) 69.
- [21] I. I. Suni, *TrAC Trends in Analytical Chemistry* **27** (2008) 604.